Human Molecular Genetics, 2018, Vol. 27, No. 1 199–210

doi: 10.1093/hmg/ddx375
Advance Access Publication Date: 10 October 2017
Association Studies Article

ASSOCIATION STUDIES ARTICLE

The biological impact of blood pressure-associated genetic variants in the natriuretic peptide receptor C gene on human vascular smooth muscle

Meixia Ren[1,2,3], Fu Liang Ng[1,2], Helen R. Warren[1,2], Kate Witkowska[1,2], Michael Baron[4], Zhilong Jia[1,5], Claudia Cabrera[1,2], Ruoxin Zhang[1], Borbala Mifsud[1], Patricia B. Munroe[1,2], Qingzhong Xiao[1], Andrea Townsend-Nicholson[4], Adrian J. Hobbs[1,2], Shu Ye[6,7,8,*,†] and Mark J. Caulfield[1,2,*,†]

[1]William Harvey Research Institute, Barts and The London School of Medicine and Dentistry and [2]National Institute for Health Research Cardiovascular Biomedical Research Unit at Barts, Barts Heart Centre, Queen Mary University of London, London, UK, [3]Fujian Key Laboratory of Geriatrics, Department of Geriatric Medicine, Fujian Provincial Hospital, Fujian Medical University, Fuzhou, China, [4]Structural & Molecular Biology, University College London, London, UK, [5]Core Laboratory of Translational Medicine, Chinese PLA General Hospital, Beijing, China, [6]Department of Cardiovascular Sciences, University of Leicester, Leicester, UK, [7]NIHR Leicester Biomedical Research Centre, Leicester, UK and [8]Shantou University Medical College, Shantou, China

*To whom correspondence should be addressed at: Department of Cardiovascular Sciences, Glenfield General Hospital, Groby Road, Leicester LE3 9QP, UK. Tel: +44 1162044754; Fax: +44 1162875792; Email: sy127@leceister.ac.uk (S.Y.); Heart Centre, William Harvey Research Institute, Charterhouse Square, London EC1M 6BQ, UK. Tel: +44 2078823402; Fax: +44 2078823408; Email: m.j.caulfield@qmul.ac.uk (M.J.C.)

Abstract

Elevated blood pressure (BP) is a major global risk factor for cardiovascular disease. Genome-wide association studies have identified several genetic variants at the *NPR3* locus associated with BP, but the functional impact of these variants remains to be determined. Here we confirmed, by a genome-wide association study within UK Biobank, the existence of two independent BP-related signals within *NPR3* locus. Using human primary vascular smooth muscle cells (VSMCs) and endothelial cells (ECs) from different individuals, we found that the BP-elevating alleles within one linkage disequilibrium block identified by the sentinel variant rs1173771 was associated with lower endogenous *NPR3* mRNA and protein levels in VSMCs, together with reduced levels in open chromatin and nuclear protein binding. The BP-elevating alleles also increased VSMC proliferation, angiotensin II-induced calcium flux and cell contraction. However, an analogous genotype-dependent association was not observed in vascular ECs. Our study identifies novel, putative mechanisms for BP-associated variants at the *NPR3* locus to elevate BP, further strengthening the case for targeting NPR-C as a therapeutic approach for hypertension and cardiovascular disease prevention.

†These authors share the senior authorship.

Received: May 30, 2017. **Revised:** September 28, 2017. **Accepted:** September 30, 2017

Introduction

As a complex quantitative trait, high blood pressure (BP) is the leading risk factor for cardiovascular disease which is influenced by genetic variation and lifestyle factors. Genome-Wide Association Studies (GWAS) in BP have shown that inter-individual variation in systolic and diastolic BP (SBP and DBP), pulse pressure (PP) and mean arterial pressure is associated with single nucleotide polymorphisms (SNPs) at the natriuretic peptide receptor C (*NPR3*) locus in different ancestries (1–4). The validated variants in the *NPR3* 3′ flanking region that link to SBP and DBP are rs1173771 in Europeans (2) and rs1173766 in East Asians and Japanese (5). Furthermore, one-third SNP in this region, rs1421811, has been associated with SBP in a population of European ancestry (6). However, the molecular and cellular basis for these genetic associations remains to be elucidated.

NPR3 encodes natriuretic peptide receptor C (NPR-C). This protein has a high affinity with all three types of natriuretic peptides (NPs). NPR-C is widely thought to function as a systemic clearance receptor that removes NPs from the circulation by facilitating NP internalization and degradation (7–9). Upregulation of NPRC in adipose and muscle tissues in obese hypertensive patients (10,11) and reduced BP in global Npr3 knockout mice (12) support a role of NPR-C as a clearance receptor in BP control. Recently, accumulated evidence has suggested NPR-C also plays a role in cell signalling coupling to G_i (13–15) and mediates some of the cardioprotective actions of NPs and their involvement in the pathogenesis of hypertension (16,17). Perhaps the best example is the identification of C-type natriuretic peptide (CNP)/NPR-C signalling as a functional pathway in the regulation of vascular tone (18). This is likely to result from CNP binding to NPR-C, stimulating G_i and activating potassium ion (K^+) conductance, leading to hyperpolarization and relaxation of vascular smooth muscle cells (VSMCs) (19). Furthermore, we have demonstrated that administration of synthetic NPR-C agonists exerts a dose-dependent and clinically valuable hypotensive impact *in vivo* (20). This is complemented by observations that $cANF^{4-23}$, a ring-deleted analogue of ANP that specifically interacts with NPR-C (7), reduces BP in spontaneously hypertensive rats (21).

There are very few studies that have functionally characterized the effects of the BP-associated variants in humans. In this study of the *NPR3* locus, we investigate whether validated SNPs influencing BP have an impact on human VSMC and endothelial cell (EC) NPR-C expression, proliferation, migration, intracellular calcium flux and cell contraction *in vitro*.

Results

Two independent BP-associated genetic signals at the NPR3 gene locus detected using a GWAS within UK Biobank

Recent publication has suggested that two independent BP-associated genetic signals exist at the *NPR3* locus (3). To determine if there were additional independent signals at this locus, we utilized the large UK Biobank (UKB) cohort (https://www.ukbiobank.ac.uk/; date last accessed October 11, 2017) with data of 140 886 individuals of European ancestry. It was observed that there were two independent, significant signals with lead SNPs rs1173727/rs7733331 [(linkage disequilibrium (LD) block 1 with published SNP rs1173771)] and rs1421811 (LD block 2) respectively at *NPR3* locus (Fig. 1A–C). The effect size and *P*-values of these BP-associated variants are shown in Table 1 (for SBP) and Supplementary Material, Table S1 (for DBP and PP). Conditional analysis (Fig. 1D) provided further validation for our approach herein that there were no additional independent signals, confirming a total of two independent signals at this locus. For example, the association of SNP rs7733331 with SBP was no longer significant ($P = 0.37$) after conditioning on the two published SNPs. Nevertheless, there was still some evidence ($P_{cond} < 1.0 \times 10^{-4}$) of residual association remaining for SNPs rs1173743 and rs1173756 (Table 1), reflecting a weak residual association existing in the rs1173771 LD block.

BP-elevating allele in rs1173771 LD block decreases NPR3 expression

To explore the effect of BP-associated SNPs on *NPR3* expression, quantitative reverse transcriptase polymerase chain reaction (qRT-PCR) was performed on primary arterial VSMCs derived from umbilical cords from different neonates ($n = 100$), an independent resource unrelated to the UKB cohort. Reduced *NPR3* mRNA levels were observed in VSMCs homozygous for the BP-elevating allele (EE) in the rs1173771 LD block, when compared with BP-lowering allele homozygous (LL) VSMCs (Fig. 2A). Consistent with the qRT-PCR results, allelic expression imbalance analysis for the 3'-UTR SNP rs1173756 ($r^2 = 0.78$ in CEU and $r^2 = 1.00$ in CHB/JPT with rs1173771) showed the BP-elevating allele (E) had lower expression levels when compared with the BP-lowering allele (L) in mRNA (Fig. 2B). Western blotting also revealed that NPR-C protein levels were lower in VSMCs of the EE genotype compared with the LL genotype (Fig. 2C). In concert, these observations strongly support a functional influence on NPR-C expression at a transcriptional level of the specific *NPR3* SNPs tested or other functional variants within the LD block.

rs1173771 and rs1173747 reside in open chromatin regions and affect nuclear protein binding

The SNPs in the rs1173771 LD block are located in non-coding regions. Bioinformatic analysis indicated some of these SNPs reside in regions with transcription regulatory features such as histone modification marks (e.g. H3K27ac) and transcriptional factor binding (Supplementary Material, Table S2). Therefore, we investigated if these SNPs had any effect on these features. Formaldehyde-assisted isolation of regulatory elements (FAIRE) followed by allelic imbalance assays in VSMCs revealed that the relative abundance of L allele versus E allele of rs1173771 (intergenic SNP in the downstream of *NPR3* gene) was significantly higher in FAIRE DNA compared with the reference DNA (Fig. 3A). Electrophoretic mobility shift assay (EMSA) with VSMC nuclear extracts demonstrated differential nuclear protein binding to the different alleles of rs1173771 (Fig. 3B). This supports the FAIRE findings that the L allele of rs1173771 is more likely to be in an open chromatin configuration and therefore be more amenable to transcription. ChIP with an anti-H3K27ac antibody followed by allelic imbalance assays of rs1173771 showed similar results (Fig. 3C). A luciferase reporter gene assay also demonstrated the L allele increased the transcriptional activity (Fig. 3D).

One intronic SNP, rs1173747, also presented an allelic difference as rs1173771 in enrichment in open chromatin (Fig. 4A), interaction with VSMCs nuclear extracts *in vitro* (Fig. 4B), and transcriptional activity (Fig. 4C), although no association between the rs1173747 flanking region with H3K27ac. These results suggest that rs1173771 and rs1173747 can modulate *NPR3* transcription by allele-dependent effects on chromatin and

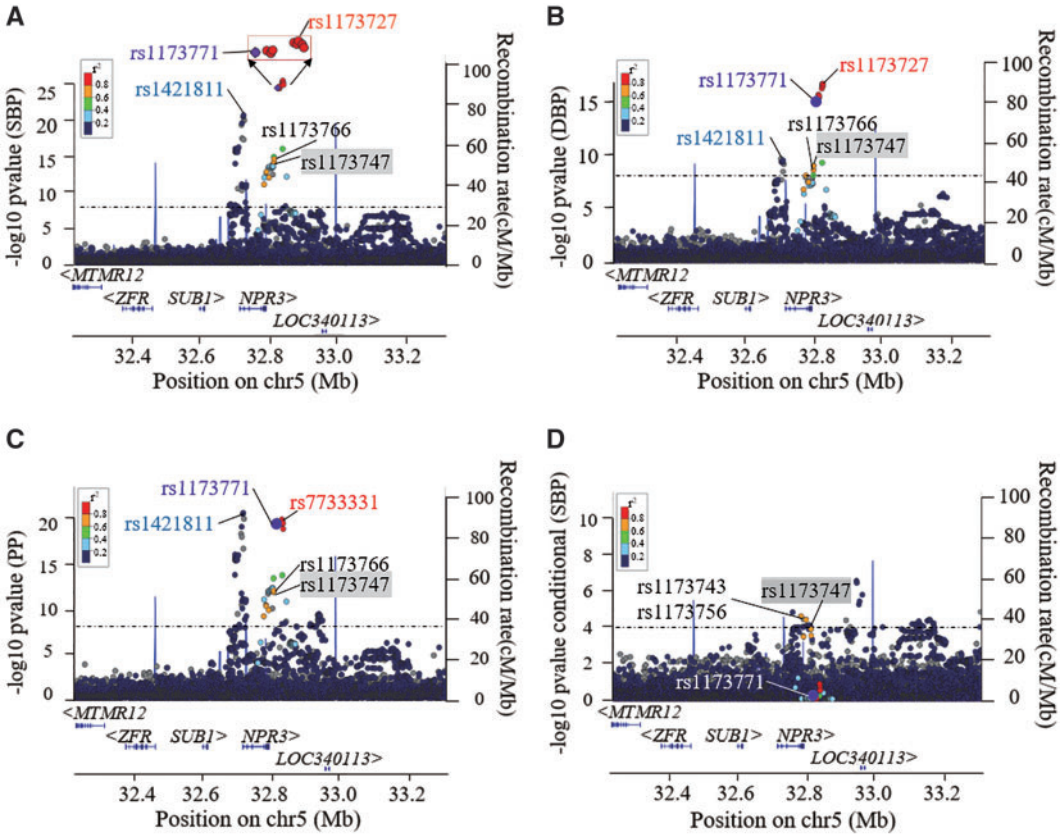

Figure 1. Regional plots for association of NPR3 variants with SBP/DBP/PP within the UK Biobank cohort. (**A–C**) Genome-wide primary association analysis of main effects for medication-adjusted SBP, DBP and PP traits using the UK Biobank cohort (*N*=140 886) showed two signals at the *NPR3* locus. The sentinel SNPs in these two independent linkage disequilibrium (LD) blocks are labelled in red or light blue text, respectively. The purple dot indicates rs1173771, the lead SNP in our previous GWAS study (2), and r^2 measures of LD are shown in relation with rs1173771. (**D**) A conditional analysis based on the two published lead SNPs, rs1173771 and rs1421811, indicated the presence of a weak residual signal with rs1173747 in the rs1173771 LD block. Note that the variants (dark blue dots) upstream of rs1173747 were not significantly associated with BP in the primary main association analysis, so are not of interest within the conditional analysis.

Table 1. Association between *NPR3* variants and blood pressure traits in UK Biobank cohort

	Candidate SNPs	Positions on Chr 5 (bp)	EA	AA	EAF	Phenotypes	SBP effect (mmHg)	*P*-value (SBP)	Conditional *P*-value (SBP)
Block 1	rs1173727	32 830 521	C	T	0.60	SBP, DBP, PP	0.75 (0.07)	3.11×10^{-26}	0.26
	rs7733331	32 828 846	C	T	0.60	SBP, DBP, PP	0.75 (0.07)	4.44×10^{-26}	0.37
	rs1173771	32 815 028	C	T	0.60	SBP, DBP, PP	0.74 (0.07)	3.26×10^{-25}	–
	rs1173766	32 804 528	C	T	0.60	SBP, DBP, PP	0.74 (0.07)	7.27×10^{-15}	2.82×10^{-4}
	rs1173747	32 782 152	A	C	0.53	SBP, DBP, PP	0.51 (0.07)	1.97×10^{-13}	6.52×10^{-4}
	rs1173756	32 789 852	C	T	0.53	SBP, DBP, PP	0.50 (0.07)	1.19×10^{-12}	9.57×10^{-5}
	rs1173743	32 775 047	T	G	0.52	SBP, PP	0.48 (0.07)	1.13×10^{-11}	6.31×10^{-5}
Block 2	rs1421811	32 714 270	C	G	0.39	SBP, DBP, PP	−0.68 (0.07)	2.15×10^{-21}	–
	rs3828591	32 713 108	G	C	0.39	SBP, DBP, PP	−0.68 (0.07)	3.55×10^{-21}	NA
	rs3762988	32 709 653	C	T	0.39	SBP, DBP, PP	−0.66 (0.07)	2.79×10^{-20}	NA
	rs7729447	32 689 773	G	A	0.32	SBP, PP	−0.58 (0.07)	1.36×10^{-14}	NA

Genetic position is based on Build 37 of a reference genome. $P<5\times10^{-8}$ was used a threshold to determine the association with BP traits. The effect is presented as unit change (mmHg) with standard error (SE) in systolic blood pressure (SBP) per copy of effect allele.

Chr, chromosome; EA, effect allele; AA, alternative allele; EAF, effect allele frequency; DBP, diastolic blood pressure; PP, pulse pressure.

transcription factor binding. UKB GWAS conditional analysis as above indicated a weak residual association ($P_{cond}<1.0\times10^{-4}$) remaining for SNPs rs1173743 and rs1173756 (both in strong LD with intronic SNP rs1173747; $r^2>0.95$) existing in the rs1173771 LD block. This provides support for our findings that rs1173771 and rs1173747 may both be acting as functional SNPs in the single LD block.

Association of BP-elevating allele with increased VSMC proliferation

To assess the potential effect of BP-associated variants on VSMC proliferation, we conducted cell counting assays using Cell Counting Kit-8 (CCK-8). We found that VSMCs carrying the E allele had an innately increased proliferation rate when compared with cells with LL (Fig. 5A), linking to allelic difference

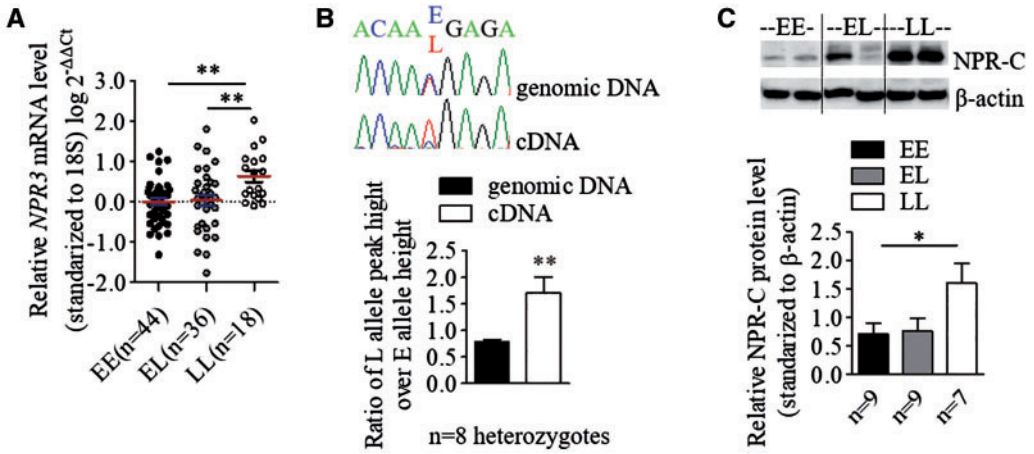

Figure 2. Blood pressure associated variants affect NPR3 expression in human VSMCs. For all panels, 'E' stands for the BP-elevating allele for each SNP, 'L' denotes the BP-lowering allele for each SNP. (**A**) Relative mRNA levels of *NPR3* in VSMCs was determined by quantitative reverse-transcription polymerase chain reaction and standardized against the reference gene 18S. Mean±SEM, $^{**}P < 0.01$. (**B**) The relative peak heights of two alleles of the 3′ UTR SNP rs1173756 (r^2=0.78 with lead SNP rs1173771) in sequencing chromatograms from genomic DNA and complementary DNA (cDNA) of VSMCs. Mean±SEM, $^{**}P < 0.01$. (**C**) A representative image of western blot analysis of NPR-C protein in VSMCs with β-actin as a loading control, Mean±SEM, $^{*}P < 0.05$.

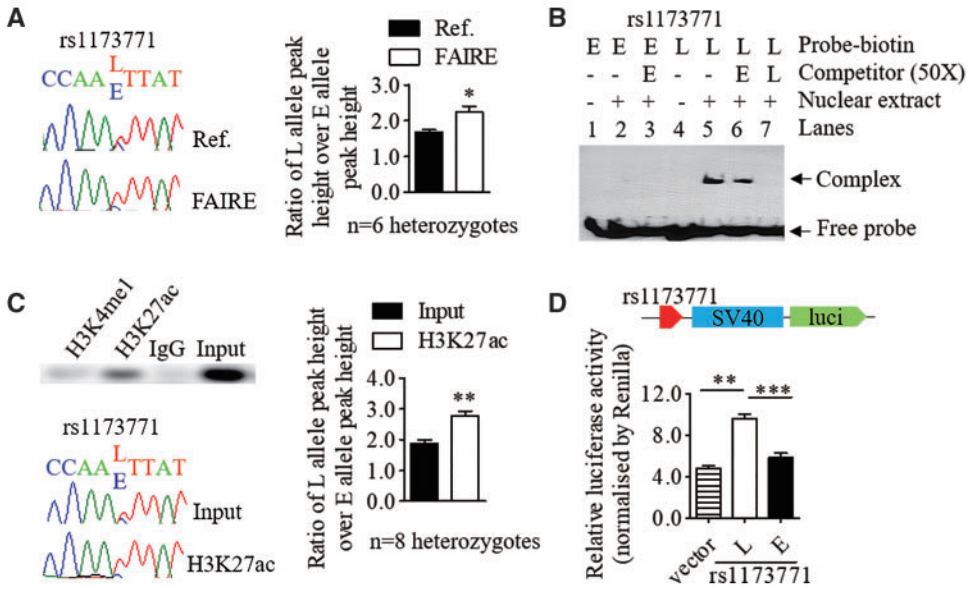

Figure 3. The BP-associated variant rs1173771 affects chromatin status and nuclear protein binding. In this figure, 'E' indicates BP-elevating allele, 'L' denotes BP-lowering allele. (**A**) Formaldehyde-assisted isolation of regulatory elements followed by allelic imbalance assay by Sanger sequencing. Left panel: Representative images showing different peak heights of the E and L alleles of rs1173771 in chromatograms derived from reference (Ref.) DNA and FAIRE DNA, respectively. Right panel: values in the bar chart are mean±SEM of *n*=6 heterozygous samples, $^{*}P < 0.05$. (**B**) Representative result of an electrophoretic mobility shift assay with the use of biotin-labelled double-stranded oligonucleotide probes and unlabelled competitors of the E and L alleles of rs11737711, and nuclear protein extracts from VSMCs. (**C**) Chromatin immunoprecipitation with an anti-H3K27ac antibody and IgG (the negative control) in heterozygous VSMCs. Upper left panel: PCR amplified DNA containing the rs1173771 site derived from anti-H3K27ac precipitated DNA, anti-H3K4me1 precipitated DNA and input DNA, respectively. Lower left panel: representative chromatographs showing the peak heights of the E and L alleles of rs1173771 from Input and precipitated DNA, respectively. Right panel: values in the bar chart are mean±SEM of seven heterozygous samples, $^{**}P < 0.01$. (**D**) Relative activity of the rs1173771 E and L alleles, respectively, in driving firefly luciferase reporter gene expression in transfected VSMCs, standardized for transfection efficiency. Mean±SEM, $^{**}P < 0.01$, $^{***}P < 0.001$.

of *NPR3* levels. Exogenous CNP (100 nmol/l) or NPR-C specific agonist cANF$^{4-23}$ (100 nmol/l) caused an equivalent genotype-dependent effect on proliferation (Fig. 5B), with a significantly greater inhibition on cells carrying LL in the presence of cANF$^{4-23}$ (Fig. 5C).

No association between NPR3 risk variants and VSMC migration

To investigate whether BP-associated *NPR3* variants influence VSMC migration, we performed *in vitro* scratch assays on primary VSMCs. However, no association was detected

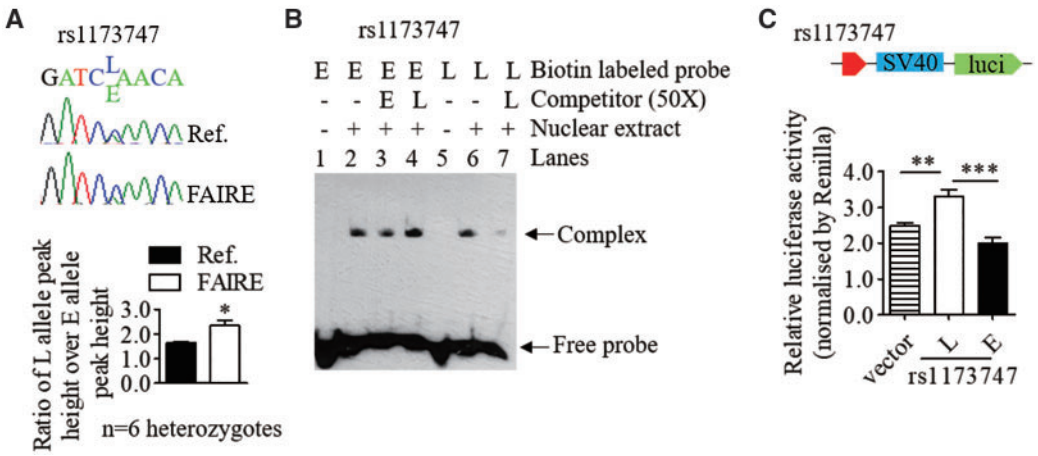

Figure 4. The BP-associated variant rs1173747 affects chromatin status and nuclear protein binding. In this figure, 'E' indicates BP-elevating allele, 'L' denotes BP-lowering allele. (**A**) Formaldehyde-assisted isolation of regulatory elements followed by allelic imbalance assays by Sanger sequencing. Representative images showing different peak heights of the E and L alleles of rs1173747 in chromatograms derived from reference (Ref.) DNA and FAIRE DNA. Mean±SEM of n=6 heterozygous samples, *P <0.05. (**B**) Representative result of electrophoretic mobility shift assay with the use of biotin-labelled double-stranded oligonucleotide probes and unlabelled competitors of the E and L alleles of rs1173747 and nuclear protein extracts from VSMCs. (**C**) Relative activity of the rs1173747 E and L alleles, respectively, in driving firefly luciferase reporter gene expression in transfected VSMCs, standardized for transfection efficiency. Mean±SEM, **P <0.01, ***P <0.001.

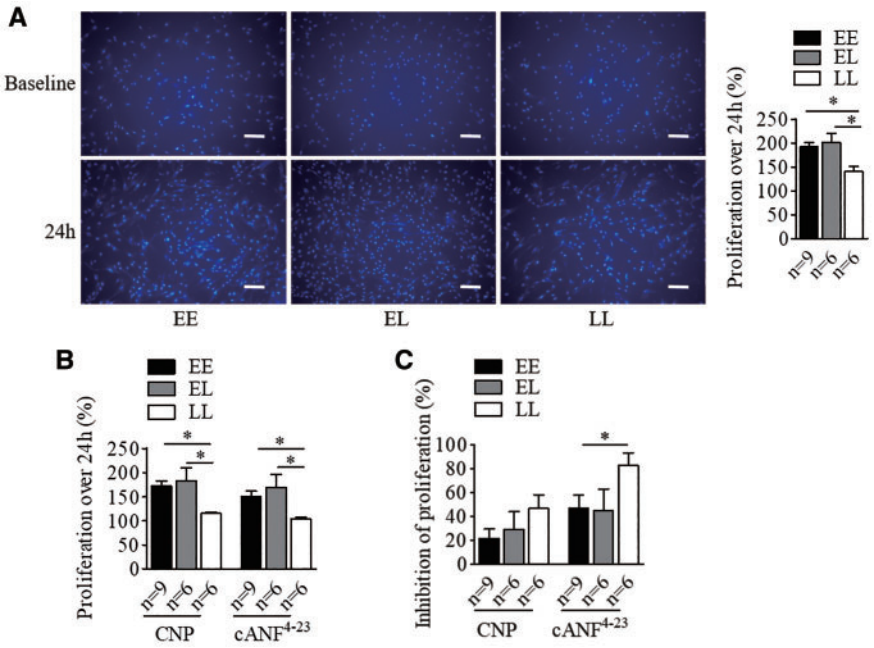

Figure 5. The BP-elevating variant at NPR3 locus is associated with increased human VSMCs proliferation. VSMCs in the absence and presence of C-type natriuretic peptide (CNP; 100 nmol/l) and the NPR-C specific agonist (cANF$^{4-23}$; 100 nmol/l) for 24 h were analysed for proliferation rate. Cell proliferation over the 24-h period was calculated as (OD450 at 24 h−OD450 at baseline)/OD450 at baseline. 'E' indicates the BP-elevating allele, 'L' denotes the BP-lowering allele. (**A**) Differences in proliferation between untreated cells of different genotypes. Representative images of DAPI stained cells of the three different genotypes at baseline and 24 h. Scale bars=200μm. Mean±SEM, *P <0.05. (**B**) Differences in proliferation between CNP or cANF$^{4-23}$ treated cells of different genotypes, and (**C**) Inhibitory effects of CNP and cANF$^{4-23}$ on proliferation of cells of different genotypes, calculated by (OD450 at 24 h of untreated cells−OD450 at 24 h of CNP-treated or cANF$^{4-23}$-treated cells)/OD450 at 24 h of untreated cells. Mean±SEM, *P <0.05.

between *NPR3* variants and cell migration (Supplementary Material, Fig. S2).

BP-elevating allele increases intracellular calcium response and cell contraction to angiotensin II in VSMCs

To evaluate the role of BP-associated variants in stimulated changes in intracellular calcium flux in VSMCs, a Fluorescent Imaging Plate Reader (FLIPR)-based calcium assay was conducted. Cells among genotypes were stimulated with angiotensin (Ang) II (10 or 100 nmol/l, representing approximate EC_{50} or EC_{90} values, respectively, see Supplementary Material, Fig. S2). We found that VSMC homozygous samples with EE exhibited an augmented intracellular calcium level along with a shorter time to peak response following stimulation with Ang II (at 10 and 100 nmol/l) in contrast to LL (Fig. 6A), indicating a

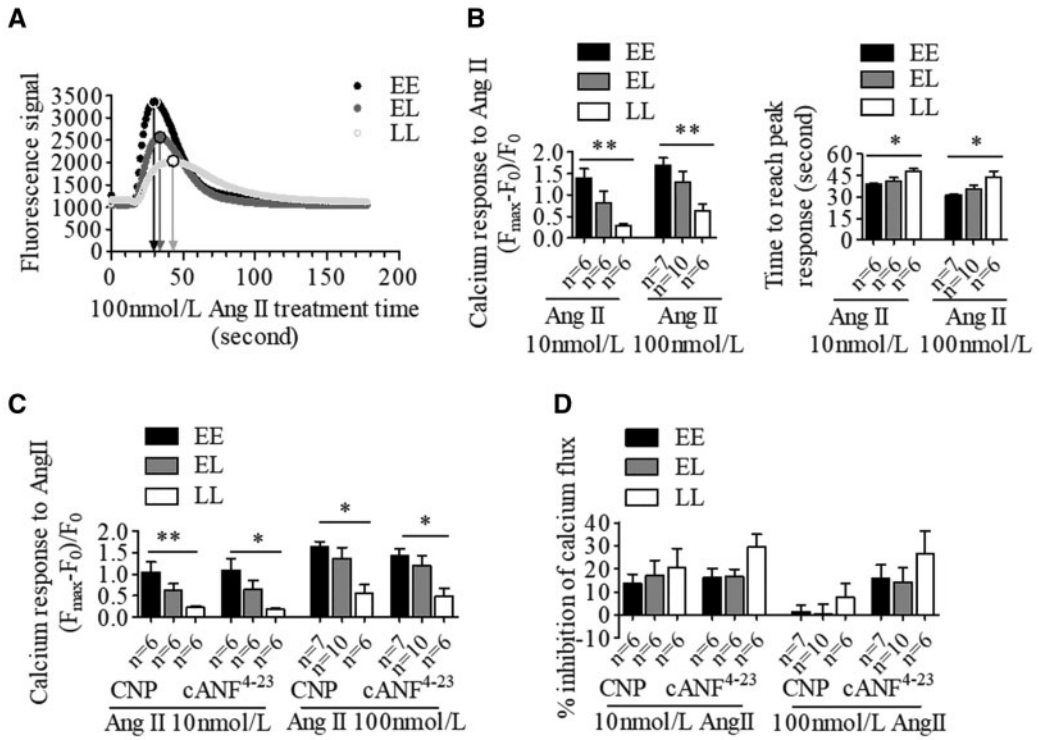

Figure 6. The BP-elevating allele at NPR3 locus increases Ang II-induced intracellular calcium changes in human VSMCs. Human VSMCs were incubated with or without C-type natriuretic peptide (CNP; 1 μmol/l) and the NPR-C specific agonist cANF$^{4-23}$(1 μmol/l), and then exposed to Ang II (10 or 100 nmol/l). 'E' indicates the BP-elevating allele, 'L' denotes the BP-lowering allele. (**A**) Representative images of intracellular calcium changes among genotypes under stimulation of 100 nmol/l Ang II. (**B**) Differences between genotypes in intracellular calcium changes in response to Ang II in the absence of CNP or cANF$^{4-23}$. Differences between genotypes in intracellular calcium level changes in response to Ang II (**C**) and drug inhibitory effect (**D**) in the presence of CNP or cANF$^{4-23}$. Mean±SEM, *P <0.05, **P <0.01.

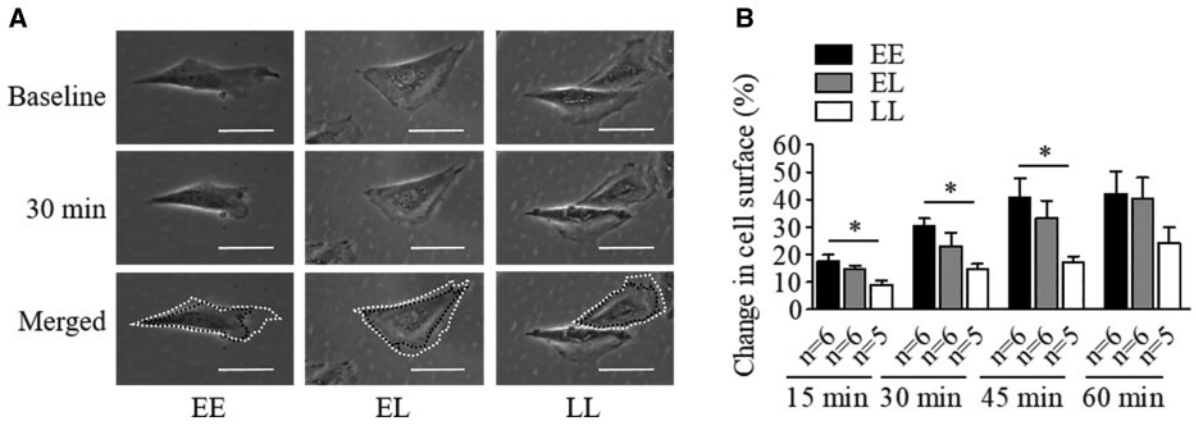

Figure 7. The BP-elevating allele at NPR3 locus enhances Ang II-induced human VSMCs contraction. 'E' indicates the BP-elevating allele, 'L' denotes the BP-lowering allele. (**A**) Representative images of VSMCs of the three different genotypes at baseline (before stimulation) and 30 min after treatment with 100 nmol/l Ang II, respectively. White dash lines show the original size of cells at baseline, and the black ones outline the sizes at 30 min in the merged panel. Scale bars = 50 μm. (**B**) Differences in 100 nmol/l Ang II stimulated VSMC contraction of different genotypes at 15, 30, 45, 60 min. Mean ± SEM, *P < 0.05.

genotype effect on intracellular calcium response to Ang II. We next examined the effect of CNP and cANF$^{4-23}$, on calcium flux. In the presence of CNP (1 μmol/l) or cANF$^{4-23}$ (1 μmol/l), VSMCs continued to exhibit the same genetic difference in Ang II-stimulated samples (Fig. 6B), with a trend towards a slightly lower effect of the BP-elevating allele samples (Fig. 6C), in accordance with our findings of allelic association of NPR-C expression level.

To investigate the potential influence of BP-associated variants in VSMC contraction, assessment of single cell contraction in response to 100 nmol/l Ang II was performed. In this setting VSMCs with EE had stronger contraction in response to Ang II

after 15, 30 and 45 min (Fig. 7), mirroring the findings linking genotype to NPR-C expression.

Association between the other (rs1421811) LD block at NPR3 gene locus and VSMCs phenotypes

We also evaluated the other independent LD block based on the SNP rs1421811. A non-significant trend was observed that the rs1421811 BP-elevating allele homozygous VSMCs (EE) had a marginally lower *NPR3* mRNA and protein level, without significant difference in cell proliferation or migration (Supplementary Material, Fig. S3). However, a higher calcium change in response to 100 nmol/l Ang II was detected in its EE (Supplementary Material, Fig. S3), consistent with the findings in rs1173711 LD block.

Effect of the BP-associated variants on vascular ECs NPR3 gene expression, and cell activities

In addition to the assays in VSMCs described above, we investigated whether the BP-associated variants in rs1173771 or rs1421811 LD block affect *NPR3* expression and cell activities in primary venous ECs derived from umbilical cords from different neonates (n = 106). Quantitative RT-PCR analysis showed that the E allele has slightly lower *NPR3* mRNA levels in ECs but without statistical significance, despite allelic expression imbalance analysis also suggested a decreased mRNA level of the E allele in rs1173771 LD block (Supplementary Material, Fig. S4). Cell viability and migration ability were also investigated and showed no significant genetic association between the *NPR3* BP-related variants in rs1173771 LD locus and these phenotypes. Whereas, the L allele in rs1421811 LD block drove a near-significant increase of *NPR3* expression and elevated cell proliferation, but not migration (Supplementary Material, Fig. S5).

Discussion

Previous genetic studies identified multiple SNPs associated with BP and hypertension susceptibility. The challenge now is to unravel the causative mechanisms and biology behind these associated gene loci. Two independent signals at the *NPR3* locus have been associated with a modest effect on BP in several studies (2,3,6). We validated both signals (with sentinel SNPs rs1173771 and rs1421811, respectively) for BP in 140 886 UKB participants and confirmed by regional conditional analysis for BP traits (SBP, DBP and PP) that the variants we have studied in these two LD blocks explain the observed association, with no additional independent signals existing.

Herein, we establish an *ex-vivo* genotype-specific human laboratory experimental strategy that reveals the biological impact of SNPs at the *NPR3* locus in VSMCs and ECs. We discovered that the BP-elevating alleles of the associated variants in rs1173771 LD block exhibit lower *NPR3* expression in VSMCs. Our findings also show that these non-coding variants (intergenic SNP rs1173771 and intronic SNP rs1173747) have an allele-dependent effects on open chromatin and transcription factor binding, thereby active transcription of *NPR3* occurring at lower levels with BP-elevating alleles, although it is also conceivable that the lower *NPR3* expression levels may be also attributable to a compensatory mechanism which attempts to diminish the NP clearance. Furthermore, our regional conditional analysis within the UKB indicates that there is a weak residual association between rs1173771 and rs1173747, implying rs1173771, rs1173747 or variants within the haplotype block might be acting as functional variants, however, the causal variant(s) and the precise mechanism behind still needs to be further identified.

In keeping with molecular, physiological and pharmacological evidence that NPR-C exerts an impact on vascular smooth muscle tone (20,22,23), we demonstrate that the BP-elevating allele homozygous cells exhibit augmented proliferation, Ang II-stimulated intracellular calcium response and cell contraction in human VSMCs. Although several models for the pathogenesis of hypertension have been proposed, there are at least two plausible mechanisms where increased VSMC proliferation and contractility can lead to raised BP: (i) increasing the vascular tone of the resistance arteries, consequently influencing systemic vascular resistance; and (ii) altering renal vascular tone and perfusion, secondarily affecting pressure-natriuresis (24,25). Taken together, these findings provide a mechanism whereby *NPR3* variants at the rs1173771 LD block could impact on BP homeostasis, through decreasing the receptor expression and subsequent modification of human VSMC reactivity (Supplementary Material, Fig. S6). In addition, functional characterization of the other independent signal with sentinel SNP rs1421811 was also undertook. An allelic-specific impact on VSMCs calcium response to a higher dose of Ang II was detected, a pattern in accord with rs1173771, supporting its genetic association with BP.

To date, the biological roles of NPR-C are not completely understood. This receptor has long been implicated in the binding, internalization and degradation of NPs (7). BP in global Npr3 knockout mice was found to be 8 mmHg lower than wild-type mice (13), which is consistent with the notion that NPR-C exerts a cardiovascular effect by mediating clearance of NPs. However, there was no change of plasma levels of NPs in the NPR-C knockout mice, which suggests that NPR-C may have other roles in addition to NP clearance. More recently, there is accumulating evidence suggesting that NPR-C has a function in intracellular signalling. For instance, it has been shown that administration of synthetic NPR-C agonists exerts a dose-dependent hypotensive impact in mice (20) and reduces the elevated BP in spontaneously hypertensive rats through inhibiting $G_{i\alpha}$ proteins and nitroxidative stress *in vivo* (21). Therefore, it is possible that NPR-C has both NP clearance and signalling functions.

With regard to its signalling function, previous studies have indicated that NPR-C supresses VSMC proliferation in response to CNP or $cANF^{4-23}$ (22,23,26). NPR-C also could reduce the L-type calcium current ($I_{Ca\text{-}L}$) via binding with CNP in mouse sinoatrial node myocytes (27), and Ang II-stimulated mesenteric artery SMC calcium flux (20). In this study, we observed such a similar inhibitory effect of CNP and $cANF^{4-23}$ on human VSMC proliferation and calcium responses to Ang II in a genotype-dependent manner, which correlates with *NPR3* gene expression levels, supporting the hypothesis that increased expression of *NPR3* in individuals enhances a protective signalling pathway. Notably, genetic differences in VSMCs proliferation, calcium flux and contraction were observed in the absence of exogenous agonist. This might be explained by the inherent production of CNP by human VSMCs in a cell culture environment (Supplementary Material, Fig. S1), although the vast majority of *in vivo* vascular CNP originates from the ECs. Another plausible explanation might be the intrinsic activity of NPR-C, which is a common facet of GPCR biology (28,29), thereby potentially generating a signal even in the absence of an agonist.

Although our study detected an effect of BP-associated SNPs on VSMCs *NPR3* expression and cell activities, we did not discern a statistically significant influence in our experiments of ECs. However, a trend was observed in some of ECs assays. For

example, ECs with the BP-lowering allele tended to have greater *NPR3* mRNA expression, and exhibited accelerated proliferation (particularly those with SNPs in the rs1421811 LD block). This is consistent with our previous work which demonstrated that NPRC stimulation by $cANF^{4-23}$ increases EC proliferation (23). Therefore, it is possible that the effect sizes were smaller in ECs and thus a large sample size would be required for the differences to reach statistical significance.

It is evident that SNPs in the protein-coding region may merely comprise 7% of complex disease-associated variants, while the majority of associated SNPs are either intronic or intergenic (30,31). To date, only a small fraction of the functional impact of complex trait variants on the development of disease have been unravelled. Our functional experiments for the intergenic SNP rs1173771 and intronic SNP rs1173747 provide one of the early examples of the mechanistic impact of associated complex trait variants at a BP level. Moreover, we show the possibility of more than one SNP acting as a functional variant in a single LD block indicating the complexity of biological impact even within one signal associated with BP.

Our study has some limitations. Although we have demonstrated that the BP-associated SNPs at the *NPR3* locus affect *NPR3* expression and VSMC function, several questions are still unclear. First, we have not determined the intracellular signalling pathways that mediate the effect of *NPR3* SNPs. Second, NPR-C is thought to be able to act as a clearance receptor and therefore it is possible that the functional *NPR3* variants could have an effect on NP clearance and consequently an influence on plasma levels of NPs. We have not investigated whether this is the case, but a previous study reported an association between a *NPR3* gene promoter SNP and plasma ANP levels in obese hypertensives (32). On the other hand, studies of NPRC-KO mice did not show changes in plasma levels of NPs but found ANP having a prolonged half-life (12). Third, it is unknown whether the decreased NPR-C expression associated with *NPR3* SNPs could in turn lead to a compensational change in the expression of NPR-B and whether the effect of *NPR3* SNPs on VSMC proliferation/calcium/contraction to Ang II could be abolished by an NPR-B antagonist. Fourth, although our study has focused on VSMCs and ECs, it is possible that the BP-associated *NPR3* SNPs may affect *NPR3* expression and NPR-C function also in other systems, such as in the autonomic or central nervous system and in skeletal growth, which may also impact on BP. These questions warrant investigations in future research.

Over 220 genetic loci have been validated that harbour variants influencing BP level and risk of hypertension (3,33–35). These newly discovered candidate genes, proteins and their related pathways can represent potential new drug targets. Here, we used a human laboratory experimental strategy to elucidate the functional impact of genetic variants associated with BP at the *NPR3* locus. Our findings in VSMCs provide compelling evidence for an important role of NPR-C in BP regulation and the development of hypertension. Furthermore, these data provide further confirmation that NPR-C should be considered as a potential therapeutic target for hypertension, and we have previously reported the efficacy of a lead compound in experimental models (20).

Materials and Methods

Genome-wide association analysis and genotype model analysis of BP traits in UKB

The full genetic data for the first ~150K UKB participants was imputed by a merged UK 10K sequencing + 1000 genomes reference panel (36). A subset of maximum of $N = 140\,886$ of unrelated Caucasian individuals with good quality data was finally analysed. Baseline characteristics and the quality control procedures see previous publication (37). We focused on data extracted from the known *NPR3* region (Chr 5: 32 214 276–33 314 487), and our SNPs of interest within the region were well imputed with very high imputation quality (INFO > 0.97). The phenotypic variable for PP was derived as SBP–DBP, per the medication-adjusted traits. A proportion (21.4%) of the UKB participants are reported to be taking anti-hypertensive medications. For these individuals, +15 mmHg was added to their SBP measurement, and +10 mmHg to DBP, by the standard adjustment convention used in all BP GWAS analyses. Exclusions such as renal and heart failure are not considered within the standard analyses.

For GWAS, linear regression analyses of the three (untransformed) continuous, medication-adjusted BP traits (SBP, DBP, PP) were performed using SNPTEST software under an additive genetic model. Each analysis included the following covariates: sex, age, age^2, BMI, top 10 PCs and UKB cohort status, where the UKB cohort status was a binary indicator. The conditional analyses within the *NPR3* region conditioning on the published SNPs were also performed using SNPTEST software, using the same phenotypic, covariates data and analysis model as for the GWAS.

Cell samples

This study had ethical approval from Queen Mary, University of London (ref: 08/H0704/140). All human tissue samples were fully anonymized before distribution to the recipient analysis groups, as per ethical approval. Primary human arterial VSMCs and venous ECs were isolated from umbilical cords from different neonates, an independent resource unrelated to the UKB cohort, using arterial media explant culture technique and collagenase digestion method, respectively, as previously described (38,39). VSMCs were cultured in Dulbecco's Modified Eagle Medium (DMEM) supplemented with 15% fetal bovine serum, while ECs were cultured in Medium 199 with supplements. The VSMCs and ECs were used in all experiments in this study, except the luciferase reporter gene assays in which a rat thoracic aorta VSMC line (A10) (ATCC, CRL-1476) was employed. Cells used in these experiments were at passage 2–6, and there were no differences between the different genotypes for each of the SNPs studied, in passage number or the level of confluency in each assay.

DNA extraction and genotyping

Genomic DNA from VSMCs and ECs was extracted using the DNeasy Blood & Tissue Kit (Promega) and genotyped by the KBiosciences Competitive Allelic-specific PCR SNP genotyping system (40). The primers used are listed in Supplementary Material, Table S3.

Quantitative reverse-transcription polymerase chain reaction

The total RNA was extracted from VSMCs and ECs, using the SV Total RNA Isolation System (Promega), then reverse transcribed into complementary DNA (cDNA) (Promega, M170). qRT-PCR for *NPR3* and *18S* (internal reference) was performed on cDNA in duplicate by using Power SYBR® Green PCR Master Mix kit (Life

Technologies) using real-time quantitative PCR instrument (ABI 7900HT machine). Primer sequences used are listed in Supplementary Material, Table S3. The expression level of *NPR3* relative to 18S from three independent experiments was then determined by the $2^{-\Delta\Delta Ct}$ method (41).

Allelic expression imbalance assay

End-point PCR for the amplification of the rs1173756 (3′-UTR SNP, highly linked with GWAS lead SNP rs1173771) flanking DNA sequence was performed on genomic DNA and cDNA, respectively, from heterozygous samples using the PCR Master Mix Kit (Novagen®). PCR products were cleaned up and then subjected to Sanger sequencing commercially at Genome Centre, Queen Mary University of London. The Peak Picker program was utilized to determine the relative peak heights of alleles in the sequencing chromatograms from genomic DNA and cDNA samples, respectively (42). Primers sequences used are listed in Supplementary Material, Table S3.

Western blot analysis

Cell lysates were quantified (Thermo Scientific, 23225), subjected to sodium-dodecyl-sulphate polyacrylamide gel electrophoresis (SDS-PAGE) and transferred to a polyvinylidene fluoride (PVDF) membrane. Blots were incubated with primary antibodies to NPR-C (1:1000 dilution, Abcam, Cat No. Ab123957) or β-actin (1:1000 dilution, Abcam, Cat No. ab 8226), respectively, followed by incubation with HRP-conjugated secondary antibody (1:3000 dilution, Cell Signaling, Cat No. #7076 S), and detected by autoradiography.

Formaldehyde-assisted isolation of regulatory elements

FAIRE was conducted according to a previous protocol (43). Heterozygous samples cells were cross-linked with 1% formaldehyde, and resuspended in lysis buffer, then sonicated to shear DNA to lengths between 200 and 800 bp (40 s sonication). The DNA lysates was subjected to phenol/chloroform/isoamyl alcohol (Sigma) to extract the open chromatin. The samples were de-crosslinked by heating and the residual proteins were digested by proteinase K (Promega). The DNA samples were subjected to allelic imbalance analysis as described above. Primer sequences used are listed in Supplementary Material, Table S3.

Chromatin immunoprecipitation

VSMCs heterozygous for SNPs rs1173771 and rs1173747 were crosslinked by 1% formaldehyde. Cells were lysed utilizing lysis buffer and the chromatin was sheared as described above. One aliquot of sheared chromatin was taken as 'Input' sample. Other aliquots were diluted with ChIP dilution buffer, and incubated with anti-human H3k27ac antibody (Abcam, Cat No. ab4729) or normal IgG (Santa Cruz, Cat No. sc-2025) overnight at 4 °C. A 10 ng Protein A/G Plus-Agarose (Santa Cruz, Cat No. sc-2003) was then added to the sample and incubated again for 3 h at 4 °C. The DNA–protein–antibody complexes bound to protein G-agarose beads were washed with washing buffers. The DNA–protein complex was eluted from the agarose by adding elution buffer, de-crosslinked, then input DNA and immunoprecipitated DNA were subjected to allelic imbalance analyses of SNPs as described above. Primer sequences used are listed in Supplementary Material, Table S3. Details of buffers utilized in this assay see Supplementary Material, Table S4.

Electrophoretic mobility shift assay

EMSA was performed as described (44). Double-stranded biotin labelled probes (10 femtomoles) were incubated with 8 μg VSMCs nuclear extracts, and/or unlabelled competitors, then subjected to non-denaturing polyacrylamide gel (6%) electrophoresis. Oligonucleotide sequences are listed in Supplementary Material, Table S3. After electrophoresis, blots were transferred to a nylon membrane (Amersham, RPN119B). The membrane was then cross-linked at 120 mJ/cm^2 for 45–60 s (Biolink, BLX-254E). Distribution of species containing nucleic acid was finally determined by a Chemiluminescent Nucleic Acid Detection Module (ThermoScientific, #89880).

Luciferase reporter gene assay

DNA fragments flanking the BP-associated variants (rs1173771 and rs1173747) (primers see Supplementary Material, Table S3) were amplified from genomic DNA and inserted upstream of the SV40 promotor between *SacI* and *MluI* in the pGL3-promotor vector (Promega). A10 cells were cultured in 24-well plates at 5×10^4/well for 24 h and then transfected with luciferase reporter gene plasmids containing DNA fragments flanking variants, along with a plasmid containing the *Renilla* luciferase gene using transfection reagents (Thermo Scientific, R0532). At 48 h post-transfection, firefly and *Renilla* luciferase activities were measured using the Dual-Luciferase Reporter Assay System (Promega, E1910). The relative firefly luciferase activity in each well was calculated with standardization to *Renilla* luciferase activity. All data came from four to six replicate wells.

Cell viability and proliferation assay

VSMCs or ECs were plated into a pre-coated 96-well plate at a density of 4000 cells/well in triplicate for each group. After overnight incubation, VSMCs were serum starved for 24 h then transferred to 15% FBS DMEM with or without 100 nmol/l CNP (Sigma-Aldrich) or cANF$^{4-23}$ (Bachem). For ECs, cells were serum starved in 0.2% BSA M199 for 4 h, then replenished with 15% FBS M199 with or without 1 nmol/l CNP or cANF$^{4-23}$. Cells were assayed at baseline under 450 nm in a microplate reader with CCK-8 reagent, a highly water-soluble tetrazolium salt, WST-8 (Dojindo, Cat No. CK04-11, Japan) and then again after a 24 h incubation with or without treatment. All experiments were conducted in triplicate, and three independent experiments were carried out for each sample in this assay. Cell proliferation over the 24-h period was calculated as (OD450 at 24 h −OD450 at baseline)/OD450 at baseline. Inhibitory effects of CNP and cANF$^{4-23}$ on proliferation of cells of different genotypes, calculated by (OD450 at 24 h of untreated cells− OD450 at 24 h of CNP-treated or cANF$^{4-23}$-treated cells)/OD450 at 24 h of untreated cells.

Enzyme immunoassay

Growth media in which VSMCs and ECs were cultured for 24 h with or without serum supplemented was collected from flasks. Detection of CNP in these cell media was performed using the commercial enzyme immunoassay (EIA) kit (Pharmaceuticals, Cat No: EK-012-03) according to the manufacturer's instructions.

The CNP concentrations in samples were calculated by non-linear regression using Graph Pad Prism version 5 (Graph Pad Software, CA, USA).

Scratch assay

The assay was carried out according to a previously published protocol (45). Cells were plated into a 24-well cell plate at a density of 10^5 cells/well for VSMCs and 1.5×10^5 cells/well for ECs to achieve a confluent monolayer, incubated overnight and serum starved as described above. A linear wound was then gently introduced in the centre of the cell monolayer using a 200 μl tip. Cells were then incubated with CNP or $cANF^{4-23}$ (both final concentrations: 100 nmol/l for VSMCs and 1 nmol/l for ECs). Images were captured at baseline, 6 h using a digital microscope camera (GXCAM-2TFT).

Calcium flux assay

VSMCs were seeded in black-wall, clear bottomed 96-well microplates at 7000 cells/well in triplicate overnight before the assay. The cells were incubated with the loading dye calcium 6 (Molecular Device, R8191) for 2 h at 37 °C. The FLIPR was pre-set to 37 °C. Freshly prepared CNP, $cANF^{4-23}$ [both final concentrations: 1 μmol/l, as in a previous study (20)] or equivolume vehicle control (double distilled water) was dispensed into wells and incubated for 10 min. Ang II (final concentrations: 10 or 100 nmol/l) was subsequently dispensed into the wells to induce calcium flux. Thereafter, the fluorescent signal was detected every second for 3 min, with the readings in the first 10 s before stimulators dispensing taken as baseline values (F_0). The intracellular calcium change was calculated using the equation $(F_{max} - F_0)/F_0$, where F_{max} was the peak value.

VSMC contraction assay

VSMC contraction was assessed by changes in planar surface under stimulation of Ang II as previously described (46,47). A 200 μL mixture with 5×10^3 cells were plated in a 35 mm × 10 mm petri dish (Corning) and incubated overnight. The cells were mounted into an onstage incubator with 5% CO_2 at 37 °C. Ang II with a final concentration of 100 nmol/l was dispensed into the dish and cells incubated for one hour. Images of the same cells were captured at 1 min before addition of Ang II, then serially every 15 min for an hour after stimulation, under phase contrast mode using a digital time-lapse microscope (Zeiss AxiVert 200 M). The planar surfaces of cells in response to Ang II were measured before and after stimulator using Image J, and calculated by the equation: $(S_{pro} - S_{post})/S_{pro}$, where S_{pro} was the cell size at 1 min before stimulation and S_{post} was the cell size after treatment at each time point. Each value of individual sample cell surface size is from six different measurement.

Statistical analyses

Data are presented as arithmetic means ± SEM. All datasets subjected to statistical analysis were compiled from three or more independent experiments, passed normality tests (KS normality test and D'Agostino & Pearson omnibus normality test), and analysed by Student's *t*-test or one-way ANOVA as appropriate using Graph Pad Prism version 5 (Graph Pad Software, CA, USA). One-way ANOVA with Bonferroni's multiple comparison test was applied to assess the statistical significance of genetic difference analysis based on *NPR3* gene expression, luciferase activity, cell proliferation, migration, calcium flux and cell contraction in response to Ang II. Student's *t*-test (two-tailed) was performed to evaluate the significance of the comparison between two alleles for AEI, FAIRE, ChIP and the genetic differences between two genotypes. Differences with $P < 0.05$ were considered statistically significant. $P < 5 \times 10^{-8}$ was used as a threshold for genome-wide significance in UKB GWAS.

Supplementary Material

Supplementary Material is available at *HMG* online.

Conflict of Interest statement. None declared.

Funding

M.J.C., M.R., H.R.W., K.W., C.C., P.B.M. and B.M. are supported by the National Institute for Health Research (NIHR) Biomedical Research Unit in Cardiovascular Disease at Barts. M.R. is the recipient of China Scholarship Council (No. 2011632047). F.L.N. is a British Heart Foundation Clinical Fellowship (FS/12/82/29736). S.Y. is supported by the British Heart Foundation (PG/16/9/31995 and RG/16/13/32609). This work falls under the portfolio of research conducted within the NIHR Leicester Biomedical Research Centre. This research has been conducted using the UK Biobank Resource. Funding to pay the Open Access publication charges for this article was provided by Queen Mary, University of London.

References

1. Flister, M.J., Tsaih, S.W., O'Meara, C.C., Endres, B., Hoffman, M.J., Geurts, A.M., Dwinell, M.R., Lazar, J., Jacob, H.J. and Moreno, C. (2013) Identifying multiple causative genes at a single GWAS locus. *Genome Res.*, **23**, 1996–2002.
2. Ehret, G.B., Munroe, P.B., Rice, K.M., Bochud, M., Johnson, A.D., Chasman, D.I., Smith, A.V., Tobin, M.D., Verwoert, G.C., Hwang, S.J. *et al.* (2011) Genetic variants in novel pathways influence blood pressure and cardiovascular disease risk. *Nature*, **478**, 103–109.
3. Surendran, P., Drenos, F., Young, R., Warren, H., Cook, J.P., Manning, A.K., Grarup, N., Sim, X., Barnes, D.R., Witkowska, K. *et al.* (2016) Trans-ancestry meta-analyses identify rare and common variants associated with blood pressure and hypertension. *Nat. Genet.*, **48**, 1151–1161.
4. Kelly, T.N., Takeuchi, F., Tabara, Y., Edwards, T.L., Kim, Y.J., Chen, P., Li, H., Wu, Y., Yang, C.-F., Zhang, Y. *et al.* (2013) Genome-wide association study meta-analysis reveals transethnic replication of mean arterial and pulse pressure loci. *Hypertension*, **62**, 853–859.
5. Kato, N., Takeuchi, F., Tabara, Y., Kelly, T.N., Go, M.J., Sim, X., Tay, W.T., Chen, C.H., Zhang, Y., Yamamoto, K. *et al.* (2011) Meta-analysis of genome-wide association studies identifies common variants associated with blood pressure variation in east Asians. *Nat. Genet.*, **43**, 531–538.
6. Johnson, T., Gaunt, T.R., Newhouse, S.J., Padmanabhan, S., Tomaszewski, M., Kumari, M., Morris, R.W., Tzoulaki, I., O'Brien, E.T., Poulter, N.R. *et al.* (2011) Blood pressure loci identified with a gene-centric array. *Am. J. Hum. Genet.*, **89**, 688–700.
7. Maack, T., Suzuki, M., Almeida, F.A., Nussenzveig, D., Scarborough, R.M., McEnroe, G.A. and Lewicki, J.A. (1987) Physiological role of silent receptors of atrial natriuretic factor. *Science*, **238**, 675–678.

8. Suga, S., Nakao, K., Hosoda, K., Mukoyama, M., Ogawa, Y., Shirakami, G., Arai, H., Saito, Y., Kambayashi, Y. and Inouye, K. (1992) Receptor selectivity of natriuretic peptide family, atrial natriuretic peptide, brain natriuretic peptide, and C-type natriuretic peptide. *Endocrinology*, **130**, 229–239.
9. Maack, T. (1996) Role of atrial natriuretic factor in volume control. *Kidney Int.*, **49**, 1732–1737.
10. Dessi-Fulgheri, P., Sarzani, R., Fau-Tamburrini, P., Tamburrini, P., Fau-Moraca, A., Moraca, A., Fau-Espinosa, E., Espinosa, E., Fau-Cola, G., Cola, G. *et al.* (1997) Plasma atrial natriuretic peptide and natriuretic peptide receptor gene expression in adipose tissue of normotensive and hypertensive obese patients. *J. Hypertens*, **15**, 1695–1699.
11. Coue, M., Badin, P.M., Vila, I.K., Laurens, C., Louche, K., Marques, M.A., Bourlier, V., Mouisel, E., Tavernier, G., Rustan, A.C. *et al.* (2015) Defective natriuretic peptide receptor signaling in skeletal muscle links obesity to type 2 diabetes. *Diabetes*, **64**, 4033–4045.
12. Matsukawa, N., Grzesik, W.J., Takahashi, N., Pandey, K.N., Pang, S., Yamauchi, M. and Smithies, O. (1999) The natriuretic peptide clearance receptor locally modulates the physiological effects of the natriuretic peptide system. *Proc. Natl. Acad. Sci. U.S.A.*, **96**, 7403–7408.
13. Anand-Srivastava, M.B. (1993) Platelets from spontaneously hypertensive rats exhibit decreased expression of inhibitory guanine nucleotide regulatory protein. Relation with adenylyl cyclase activity. *Circ. Res.*, **73**, 1032–1039.
14. Anand-Srivastava, M.B., Sairam, M.R. and Cantin, M. (1990) Ring-deleted analogs of atrial natriuretic factor inhibit adenylate cyclase/cAMP system. Possible coupling of clearance atrial natriuretic factor receptors to adenylate cyclase/cAMP signal transduction system. *J. Biol. Chem.*, **265**, 8566–8572.
15. Anand-Srivastava, M.B., Srivastava, A.K. and Cantin, M. (1987) Pertussis toxin attenuates atrial natriuretic factor-mediated inhibition of adenylate cyclase. Involvement of inhibitory guanine nucleotide regulatory protein. *J. Biol. Chem.*, **262**, 4931–4934.
16. Gilman, A.G. (1987) G-proteins—transducers of receptor-generated signals. *Ann Rev. Biochem.*, **56**, 615–649.
17. Anand-Srivastava, M.B. (2005) Natriuretic peptide receptor-C signaling and regulation. *Peptides*, **26**, 1044–1059.
18. Villar, I.C., Panayiotou, C.M., Sheraz, A., Madhani, M., Scotland, R.S., Nobles, M., Kemp-Harper, B., Ahluwalia, A. and Hobbs, A.J. (2007) Definitive role for natriuretic peptide receptor-C in mediating the vasorelaxant activity of C-type natriuretic peptide and endothelium-derived hyperpolarising factor. *Cardiovasc. Res.*, **74**, 515–525.
19. Chauhan, S.D., Nilsson, H., Ahluwalia, A. and Hobbs, A.J. (2003) Release of C-type natriuretic peptide accounts for the biological activity of endothelium-derived hyperpolarizing factor. *Proc. Natl. Acad. Sci. U.S.A.*, **100**, 1426–1431.
20. Moyes, A.J., Khambata, R.S., Villar, I., Bubb, K.J., Baliga, R.S., Lumsden, N.G., Xiao, F., Gane, P.J., Rebstock, A.-S., Worthington, R.J. *et al.* (2014) Endothelial C-type natriuretic peptide maintains vascular homeostasis. *J. Clin. Invest.*, **124**, 4039–4051.
21. Li, Y., Sarkar, O., Brochu, M. and Anand-Srivastava, M.B. (2014) Natriuretic peptide receptor-C attenuates hypertension in spontaneously hypertensive rats: role of nitroxidative stress and Gi proteins. *Hypertension*, **63**, 846–855.
22. Li, Y., Hashim, S. and Anand-Srivastava, M.B. (2006) Intracellular peptides of natriuretic peptide receptor-C inhibit vascular hypertrophy via Gqalpha/MAP kinase signaling pathways. *Cardiovasc. Res.*, **72**, 464–472.
23. Khambata, R.S., Panayiotou, C.M. and Hobbs, A.J. (2011) Natriuretic peptide receptor-3 underpins the disparate regulation of endothelial and vascular smooth muscle cell proliferation by C-type natriuretic peptide. *Br. J. Pharmacol.*, **164**, 584–597.
24. Mendelsohn, M.E. (2005) In hypertension, the kidney is not always the heart of the matter. *J. Clin. Invest.*, **115**, 840–844.
25. Montani, J.P. and Van Vliet, B.N. (2009) Understanding the contribution of Guyton's large circulatory model to long-term control of arterial pressure. *Exp. Physiol.*, **94**, 382–388.
26. El Andalousi, J., Li, Y., Anand-Srivastava, M.B. and Komarova, Y. (2013) Natriuretic peptide receptor-C agonist attenuates the expression of cell cycle proteins and proliferation of vascular smooth muscle cells from spontaneously hypertensive rats: role of Gi proteins and MAPkinase/PI3kinase signaling. *PLoS One*, **8**, e76183.
27. Rose, R.A., Lomax, A.E. and Giles, W.R. (2003) Inhibition of L-type Ca2+ current by C-type natriuretic peptide in bullfrog atrial myocytes: an NPR-C-mediated effect. *Am. J. Physiol. Heart Circ. Physiol.*, **285**, H2454–H2462.
28. de Ligt, R.A., Kourounakis, A.P. and Ijzerman, A.P. (2000) Inverse agonism at G protein-coupled receptors: (patho)physiological relevance and implications for drug discovery. *Br. J. Pharmacol.*, **130**, 1–12.
29. Costa, T. and Cotecchia, S. (2005) Historical review: negative efficacy and the constitutive activity of G-protein-coupled receptors. *Trends Pharmacol. Sci.*, **26**, 618–624.
30. Hindorff, L.A., Sethupathy, P., Junkins, H.A., Ramos, E.M., Mehta, J.P., Collins, F.S. and Manolio, T.A. (2009) Potential etiologic and functional implications of genome-wide association loci for human diseases and traits. *Proc. Natl. Acad. Sci. U.S.A.*, **106**, 9362–9367.
31. Pennisi, E. (2011) The biology of genomes. Disease risk links to gene regulation. *Science*, **332**, 1031.
32. Sarzani, R., Dessi-Fulgheri, P., Fau-Salvi, F., Salvi, F., Fau-Serenelli, M., Serenelli, M., Fau-Spagnolo, D., Spagnolo, D., Fau-Cola, G., Cola, G. *et al.* (1999) A novel promoter variant of the natriuretic peptide clearance receptor gene is associated with lower atrial natriuretic peptide and higher blood pressure in obese hypertensives. *J. Hypertens*, **17**, 1301–1305.
33. Witkowska, K., Ren, M. and Caulfield, M. (2015) Early vascular aging (EVA). In Nilsson, P., Olsen, M., Laurent, S. (eds), *New Directions in Cardiovascular Protection*. Academic Press, London, UK, pp. 239–260.
34. Ehret, G.B., Ferreira, T., Chasman, D.I., Jackson, A.U., Schmidt, E.M., Johnson, T., Thorleifsson, G., Luan, J.A., Donnelly, L.A. and Kanoni, S. (2016) The genetics of blood pressure regulation and its target organs from association studies in 342, 415 individuals. *Nat. Genet.*, **48**, 1171–1184.
35. Wain, L.V., Vaez, A., Jansen, R., Joehanes, R., van der Most, P.J., Erzurumluoglu, A.M., O'Reilly, P.F., Cabrera, C.P., Warren, H.R., Rose, L.M. *et al.* (2017) Novel blood pressure locus and gene discovery using genome-wide association study and expression data sets from blood and the kidney. *Hypertension* **70**, e4–e19. DOI: 1161/HYPERTENSIONAHA.117.09438.
36. Horikoshi, M., Beaumont, R.N., Day, F.R., Warrington, N.M., Kooijman, M.N., Fernandez-Tajes, J., Feenstra, B., van Zuydam, N.R., Gaulton, K.J., Grarup, N. *et al.* (2014) Genome-wide associations for birth weight and correlations with adult disease. *Hypertension*, **43**, 837–840.
37. Warren, H.R., Evangelou, E., Cabrera, C.P., Gao, H., Ren, M., Mifsud, B., Ntalla, I., Surendran, P., Liu, C., Cook, J.P. *et al.* (2017) Genome-wide association analysis identifies novel

blood pressure loci and offers biological insights into cardiovascular risk. *Nat. Genet.*, **49**, 403–415.
38. Leik, C.E., Willey, A., Graham, M.F. and Walsh, S.W. (2004) Isolation and culture of arterial smooth muscle cells from human placenta. *Hypertension*, **43**, 837–840.
39. Grobmyer, S.R., Kuo, A., Orishimo, M., Okada, S.S., Cines, D.B. and Barnathan, E.S., (1993) Determinants of binding and internalization of tissue-type plasminogen activator by human vascular smooth muscle and endothelial cells. *J. Biol. Chem.*, **268**, 13300.
40. Saxena, R.K., Penmetsa, R.V., Upadhyaya, H.D., Kumar, A., Carrasquilla-Garcia, N., Schlueter, J.A., Farmer, A., Whaley, A.M., Sarma, B.K., May, G.D. *et al.* (2012) Large-scale development of cost-effective single-nucleotide polymorphism marker assays for genetic mapping in pigeonpea and comparative mapping in legumes. *DNA Res.*, **19**, 449–461.
41. Livak, K.J. and Schmittgen, T.D. (2001) Analysis of relative gene expression data using real-time quantitative PCR and the 2(-Delta Delta C(T)) method. *Methods*, **25**, 402–408.
42. Ge, B., Gurd, S., Gaudin, T., Dore, C., Lepage, P., Harmsen, E., Hudson, T.J. and Pastinen, T. (2005) Survey of allelic expression using EST mining. *Genome Res.*, **15**, 1584–1591.
43. Simon, J.M., Giresi, P.G., Davis, I.J. and Lieb, J.D. (2012) Using formaldehyde-assisted isolation of regulatory elements (FAIRE) to isolate active regulatory DNA. *Nat. Protoc.*, **7**, 256–267.
44. Hellman, L.M. and Fried, M.G. (2007) Electrophoretic mobility shift assay (EMSA) for detecting protein–nucleic acid interactions. *Nat. Protoc.*, **2**, 1849–1861.
45. Liang, C.-C., Park, A.Y. and Guan, J.-L. (2007) In vitro scratch assay: a convenient and inexpensive method for analysis of cell migration in vitro. *Nat. Protoc.*, **2**, 329–333.
46. Li, Q.-F. and Tang, D.D. (2009) Role of p47(phox) in regulating Cdc42GAP, vimentin, and contraction in smooth muscle cells. *Am. J. Physiol. Cell Physiol.*, **297**, C1424–C1433.
47. Du, J., Sours-Brothers, S., Coleman, R., Ding, M., Graham, S., Kong, D.-H. and Ma, R. (2007) Canonical transient receptor potential 1 channel is involved in contractile function of glomerular mesangial cells. *J. Am. Soc. Nephrol.*, **18**, 1437–1445.